Ppb-level H_2S detection for SF_6 decomposition based on a fiber-amplified telecommunication diode laser and a background-gas-induced high-*Q* photoacoustic cell

Xukun Yin,[1,2] Lei Dong,[1,2,a)] Hongpeng Wu,[1,2] Weiguang Ma,[1,2] Lei Zhang,[1,2] Wangbao Yin,[1,2] Liantuan Xiao,[1,2] Suotang Jia,[1,2] and Frank K. Tittel[3]
[1]*State Key Laboratory of Quantum Optics and Quantum Optics Devices, Institute of Laser Spectroscopy, Shanxi University, Taiyuan 030006, China*
[2]*Collaborative Innovation Center of Extreme Optics, Shanxi University, Taiyuan 030006, China*
[3]*Department of Electrical and Computer Engineering, Rice University, Houston, Texas 77005, USA*

(Received 8 June 2017; accepted 8 July 2017; published online 19 July 2017)

A ppb-level hydrogen sulfide (H_2S) gas sensor for sulfur hexafluoride (SF_6) decomposition analysis was developed by means of a background-gas-induced high-*Q* differential photoacoustic cell (PAC) and a fiber-amplified telecommunication diode laser. The watt-level excitation laser power compensates the sensitivity loss as a result of using a low cost, near-IR laser source. The differential design with a large cylindrical resonator diameter allows the PAC to accommodate the high power beam and maintain a low noise level output. The theory of background-gas-induced high-*Q* PAC is provided and was verified experimentally. A H_2S detection limit (1σ) of 109 ppb in a SF_6 buffer gas was achieved for an averaging time of 1 s, which corresponds to a normalized noise equivalent absorption coefficient of $2.9 \times 10^{-9}\,cm^{-1}\,W\,Hz^{-1/2}$. *Published by AIP Publishing.*
[http://dx.doi.org/10.1063/1.4987008]

Sulfur hexafluoride (SF_6) gas has an excellent insulating property, which is widely used as an insulating medium in electric power systems, such as gas circuit breakers (GCBs), gas-insulated switchgears (GIS), transformers (GIT), and transmission pipes (GIL).[1–3] Normally, SF_6 is hard to decompose, but in the case of superheating and a partial discharge (PD) caused by latent inner insulation defects, a portion of SF_6 gas molecules are decomposed. For consecutive reactions with contaminants such as water vapor and oxygen, various chemical byproducts, such as H_2S, SO_2, SF_4, CO, CF_4, and SOF_2, are generated which can chemically attack solid insulation materials and accelerate insulation aging and eventually lead to power system failure. Hence, the trace gas analysis for SF_6 decomposition as a powerful diagnostic technique was developed to determine the status and identify the reasons for PD to occur in electrical power equipment. In particular, it was recognized that H_2S and SO_2 contents can effectively determine the insulation condition of the electrical equipment.[3] Therefore, there is considerable interest in developing a sensitive, selective, and cost-effective sensor for H_2S detection in a SF_6 buffer gas environment.

The sensitivity requirement for H_2S detection in SF_6 decomposition analysis is usually <1 ppm. To date, there are no commercially available H_2S sensors meeting this requirement. However, many photoacoustic spectroscopy (PAS)[4–12] based H_2S gas sensors with nitrogen (N_2) as the buffer gas were reported due to their excellent characteristics such as high sensitivity, fast response, and compact size. In 2013, Szabó *et al.*[13] demonstrated a PAS based H_2S detector in the near-IR wavelength region and obtained a minimum detectable limit of 6 ppmv ($3\,\sigma$) with an integration time of 10 s. A ppm-level detection sensitivity is not sufficient for the SF_6 decomposition detection. The selection of a stronger H_2S absorption band in the mid-IR wavelength region has the potential to improve the detection limit. Recently, several quartz-enhanced photoacoustic spectroscopy (QEPAS) based H_2S sensors were reported using mid-IR[14,15] and THz[16] laser sources, reducing the H_2S detection limit from a ppm level down to a sub-ppm level. An increase in incident optical power in PAS is an alternative to improve the detection limit due to the PAS linear relationship between sensitivity and excitation optical power. In 2015, Wu *et al.*[17,18] combined a fiber-amplified near-IR laser diode with the QEPAS technique, resulting in a H_2S sensor with the detection sensitivity of hundreds of ppb in N_2. QEPAS based sensors have a small size and excellent performance and detect trace H_2S gas in a N_2 buffer gas. The high sensitivity obtained by a QEPAS sensor is due to the inherent high quality factor (*Q*-factor) of a quartz tuning fork (QTF), which is the resonant acoustic transducer in QEPAS. However, the vibration damping coefficient of the QTF dramatically increases when a QTF is exposed to the heavier density SF_6, leading to a <5 times lower *Q*-factor.[19] As a result, the QEPAS technique is no longer valid in trace gas analysis for SF_6 decomposition. Instead, a resonant photoacoustic cell (PAC) with a SF_6 buffer gas possesses a higher *Q*-factor due to the fact that several SF_6 physical constants strongly differ from those of N_2. The parameters occur in the expression of the quality factor (density, thermal conductivity, molar mass, specific heat, and viscosity) and determine its value.

In this paper, we report a PAS based sensor system for H_2S detection in SF_6 buffer gas. A near-IR telecommunication diode laser was employed to reduce the cost, and its power was boosted up to ~1.4 W by means of a low-cost, erbium-doped optical fiber amplifier (EDFA). The optical power of ~1.4 W was two orders of magnitude higher than the seed

a)Electronic mail: donglei@sxu.edu.cn

TABLE I. Physical constants of SF_6 and N_2 gases at 20 °C and 1 atm.

Buffer gas	Velocity (m/s)	ρ_0 (kg/m^3)	γ	M (kg/mol)	μ (Pa/s)	κ [W/(mK)]	c_p [J/(mol K)]	Q
SF_6	133	6.52	1.1	0.146	1.53×10^{-5}	0.013	97.5	81
N_2	340	1.16	1.4	0.028	1.75×10^{-5}	0.026	29.1	38

optical power, thus compensating for the sensitivity loss due to the weak H_2S absorption line strength in the near-IR wavelength region. A differential PAC was designed, which has a ~4 times higher quality factor in SF_6 than in N_2. As a result, a ppb-level SF_6 detection sensitivity was achieved.

The amplitude S of the photoacoustic signal is related to the cell constant C, the incident optical power P_0, and the molecular absorption coefficient α, i.e., $S = C\alpha P_0$.[20] Hence, there are three ways to enhance the signal amplitude using (i) a larger cell constant, (ii) a stronger absorption coefficient, or (iii) a higher optical power. The cell constant describes the sensitivity of the photoacoustic resonator at its resonance frequency, which depends on the resonator size (radius R_C and length L_C), the resonance frequency f, and the resonator Q-factor, as well as the spatial overlap of the laser beam and the standing acoustic wave pattern F. In the case of identical resonator sizes, α, P_0, and F, the ratio R of the signal amplitude S in SF_6 and N_2 can be expressed as

$$\frac{S_{SF_6}}{S_{N_2}} = \frac{C_{SF_6}}{C_{N_2}} = \frac{(\gamma_{SF_6} - 1)Q_{SF_6} f_{N_2}}{(\gamma_{N_2} - 1)Q_{N_2} f_{SF_6}}, \quad (1)$$

where γ is the ratio of the specific heats at constant pressure and constant volume.

The resonator Q-factor describes the energy losses during one period in the acoustic wave propagation, which has different origins. In the case of a resonant PAC, the most important contribution comes from the viscous and thermal losses, which are characterized by the so-called viscous boundary layer thickness $d_v = (\mu/\rho_0 \pi f)^{1/2}$ and thermal boundary layer thickness $d_h = (\kappa M/c_p \rho_0 \pi f)^{1/2}$, where μ is the gas viscosity, ρ_0 is the gas density, κ is the gas thermal conductivity, M is the molar mass of the target gas molecule, and c_p is the gas mixture specific heat at constant pressure.[21] The contribution of the losses to the Q-factor for a longitudinal resonance can be expressed as

$$Q = \frac{R_c}{d_\nu + (\gamma - 1)d_h(1 + 2R_c/L_c)}. \quad (2)$$

The Q-factor can be obtained by substituting the physical constants of the N_2 and SF_6 buffer gases at 20 °C and 1 atm. These constants are listed in Table I. For a 90 mm long cylindrical resonator with a 6 mm diameter, theoretical Q values of 81 and 38 were obtained for SF_6 and N_2 buffer gases, respectively. The Q-factor of the resonator in SF_6 shows a gain factor of 2 due to the background gas inducement, which changes the low-Q resonator in N_2 to a high-Q resonator in SF_6.[22] A high Q-factor is helpful to enhance the signal amplitude based on Eq. (1).

A schematic diagram of a PAS based H_2S sensor system is depicted in Fig. 1. A 20 mW telecommunication distributed feedback (DFB) laser (FITEL, model FRL 15DCWD) was used to reduce the sensor system cost, whose wavelength could be tuned from 1562 nm to 1582 nm. This laser was mounted onto a driver board to control both the DFB laser current and temperature. The current was modulated by a function generator (Agilent, model 33500B) at $f_0/2$, where f_0 is the resonant frequency of the PAC. The modulated laser beam was directed to an EDFA (Connect laser technology, model MFAS-L-EY-B-MP), which is used to boost the incident optical power. The output laser beam from the EDFA with an output power of 1.36 W was directed to a fiber collimator (OZ optics, model LPC-01) and then passed through a differential PAC. The PAC had two identical cylindrical resonators, each of which was 6×90 mm in size. Two custom 6 mm-diameter electret condenser microphones with a sensitivity of -32 dB ± 3 dB at 1 kHz were mounted on the walls in the middle of each resonator to detect the photoacoustic signals. The signals from the two microphones are differentially amplified. As a result, all noise components that are coherent in the two resonators and microphones, such as the flow, window noise, and external electromagnetic disturbance, are effectively suppressed, and thus, the signal-to-noise ratio (SNR) of the reported sensor system is increased.[23] The differential signals were amplified by a transimpedance amplifier (TA) and then fed into a lock-in amplifier (Stanford research system, model SR830), which was used to demodulate the signals at $2f$ harmonics. The lock-in amplifier was set to a time constant of 1 s and 12 dB/oct filter slope, corresponding to a detection bandwidth of 0.25 Hz.

A gas dilution system (Environics, model EN4000) was used to generate different concentrations of H_2S in N_2 or SF_6 buffer gas. A sampling system containing a diaphragm pump

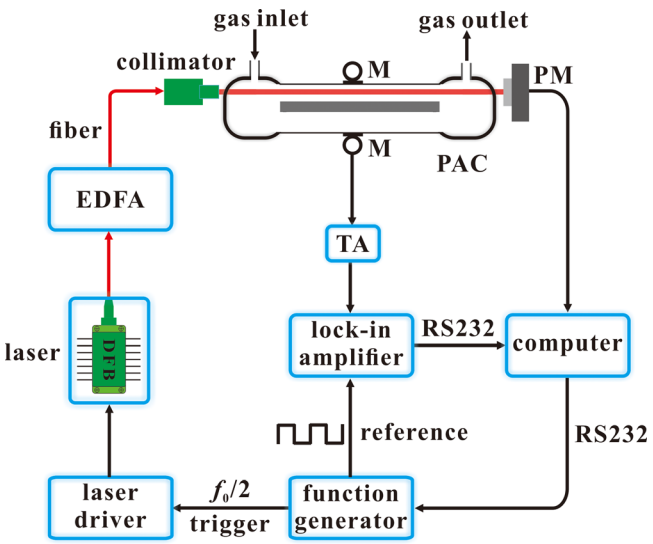

FIG. 1. Schematic of the PAS based H_2S sensor system using a differential photoacoustic cell and a fiber amplified diode laser. EDFA: erbium-doped fiber amplifier; PAC: photoacoustic cell; PM: power meter; M: microphone, and TA: transimpedance amplifier.

(KNF technology, model N813.5ANE), a pressure controller (ALICAT, model SL030), and a needle valve was used to control and maintain the sensor system pressure and gas flow. The gas flow rate was set at a constant value of 70 sccm for our experimental analysis.

The interference-free H_2S absorption line at 6320.6 cm^{-1} was selected as the target line with a line strength of 1.056×10^{-22} cm/molecule. The laser temperature was set to 31.6 °C. A 2*f* wavelength-modulation spectroscopy (2*f*-WMS) technology was employed to obtain the H_2S photoacoustic signals ranging from 6320 cm^{-1} to 6322 cm^{-1} by scanning the laser current as shown in Fig. 2. The column lines at the bottom of Fig. 2 indicate the strengths and positions of the H_2S absorption lines, which were obtained from the HITRAN database.[24] The 25 ppm H_2S/SF_6 gas mixtures were then introduced into the PAC, and the 2*f* photoacoustic signals at 400 Torr and 700 Torr were obtained at the optimum current modulation depths of 8 mA and 20 mA, respectively. At pressures $P < 400$ Torr, discrete 2*f* photoacoustic signals can be observed, while at pressures $P > 700$ Torr, the targeted line merges with its weaker neighbor at 6320.5 cm^{-1}, yielding a stronger 2*f* signal. Therefore, the operating pressure of the sensor was set to 700 Torr in the following experiments.

The characteristics of the differential PAC filled with SF_6 and N_2 buffer gases were investigated. The wavelength of the telecommunication diode laser remained at the peak of the SF_6 target line. The modulation frequency was scanned in order to obtain the PAC response curves in N_2 and SF_6 buffer gases as shown in Fig. 3. The measured resonance frequencies of the cell were $f_{N_2} = 2f_1 = 1772.6$ Hz and $f_{SF_6} = 2f_2 = 686.8$ Hz. The *Q*-factor can be experimentally obtained from the ratio of the resonance frequency to the half-width value of the resonance profile, which yielded calculated *Q*-factors of 22 and 84, respectively, in the N_2 and SF_6 buffer gases. The experimentally obtained *Q*-factor, in the case of the SF_6 buffer gas, is in excellent agreement with the theoretical value of 81 in Table I. In the case of N_2, the discrepancy between the theoretical and experimental values is due to the fact that the response curve of a low-*Q* resonator is a complex function of several eigenmodes[22] and therefore cannot be determined with sufficient accuracy. Hence, the response curve has to be determined experimentally. As a result of our measurements, the *Q*-factor of the resonator in SF_6 has a gain factor of 4 compared to that in N_2, instead of the calculated gain factor of 2. Substituting the obtained parameters into Eq. (1), a ratio *R* of 2.3 was calculated, which implies that the signal amplitude in the SF_6 buffer gas is ~2 times larger than in the N_2 buffer gas when an identical PAC, target absorption line, and excitation optical power are used.

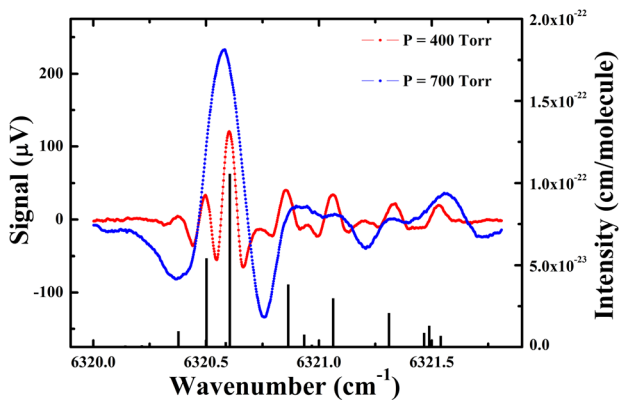

FIG. 2. Second-harmonic H_2S signals range from 6320 cm^{-1} to 6322 cm^{-1} obtained by scanning the laser current. The signals were acquired at 400 (red) and 700 Torr (blue). The H_2S absorption line strengths and positions from the HITRAN database (black) are also shown.

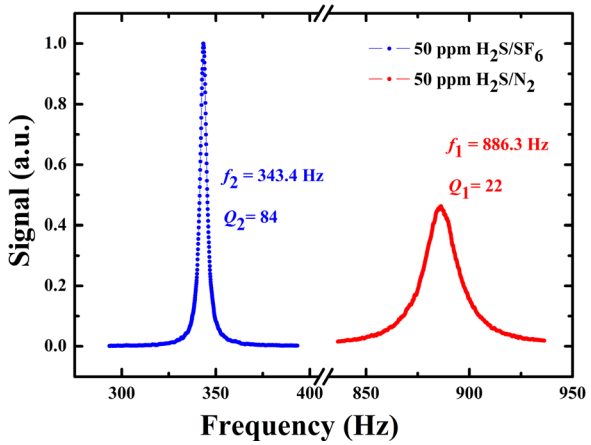

FIG. 3. Resonance frequency response curves of the differential photoacoustic cell for 50 ppm H_2S in SF_6 (blue) and N_2 (red) buffer gases.

The measured SNRs as a function of the powers are plotted in Fig. 4 in order to verify the relationship between the incident optical power and the SNR since increasing the incident optical power improved the detection limit. A H_2S concentration of 25 ppm was used. Noise levels were defined as the standard deviations (1σ) of the output signals with different incident optical powers in pure SF_6 buffer gas. A linear fitting routine was implemented. The obtained *R*-square value of 0.9998 indicates that the SNR increases linearly with increasing incident optical power. Further evaluation tests were performed at an incident optical power of 1.36 W in order to obtain the highest H_2S detection sensitivity in SF_6.

The power-boosted H_2S sensor with a gas-induced high-*Q* differential PAC in SF_6 buffer gas was evaluated with different H_2S concentrations. The measurements were carried

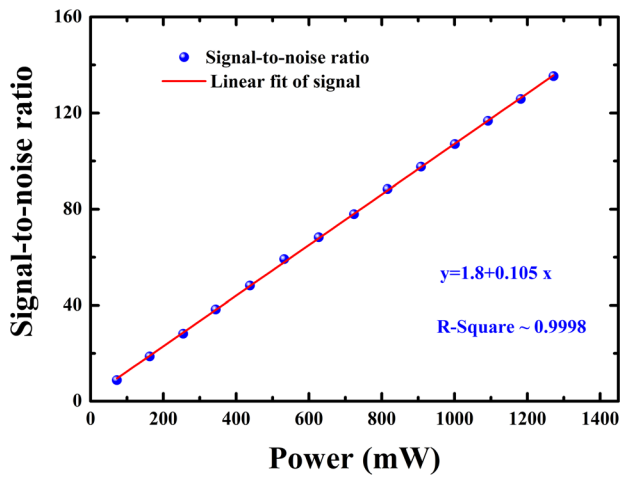

FIG. 4. Power-boosted PAS signal-to-noise ratio as a function of the actual power measured after the photoacoustic cell.

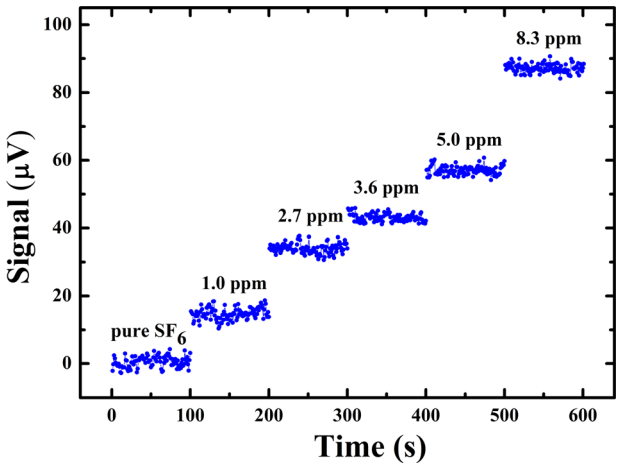

FIG. 5. Time sequence of concentration measurements for pure SF_6 and five different H_2S concentrations.

out at atmospheric pressure and room temperature. Figure 5 shows the time sequence of the concentration measurements for pure SF_6 and five different H_2S concentrations. The signal amplitudes were recorded continuously for 100 s with the laser excitation wavelength being locked at the center of the target H_2S absorption line. As shown in Fig. 5, a noise level of 1.6 μV was observed for pure SF_6. For a 1 ppm H_2S/SF_6 gas mixture, a signal of 14.7 μV $\pm$ 1.6 μV was obtained, and hence, the SNR is 9.2. The detection limit (1σ) is 109 ppb for an averaging time of 1 s, which corresponds to a normalized noise equivalent absorption (NNEA) coefficient of $2.9 \times 10^{-9}\,\mathrm{cm^{-1}W\,Hz^{-1/2}}$. A similar experimental assessment was implemented for a N_2 buffer gas. In this case, the detection limit (1σ) was 281 ppb for an averaging time of 1 s, which is 2.6 times worse than that for SF_6. The ratio R of the signal amplitude S in SF_6 and N_2 is in excellent agreement with our theoretical prediction.

In conclusion, a ppb-level PAS H_2S sensor for SF_6 decomposition analysis was developed and demonstrated. The special features of SF_6 gas result in a high-Q resonator for a SF_6 buffer gas as compared to a low-Q resonator in the case of a N_2 buffer gas. As a result, the H_2S signal amplitude in SF_6 was improved by a factor of 2.6 compared to using N_2 as the buffer gas. The strength of the selected near-IR absorption line is $\sim$10 times weaker than the absorption line in the mid-IR spectral regions but was compensated by means of a fiber-amplified incident optical power. The differential design of the PAC with a relatively large resonator diameter is capable of suppressing the noise and accommodates the high-power excitation source. These three factors work together and result in a detection limit of 109 ppb for an averaging time of 1 s, which is $\sim$7 times better than a previously reported QEPAS based H_2S sensor in N_2 buffer gas.[17] Further improvements of the detection sensitivity can be made either by enhancing the incident optical power or by reducing the resonator volume in order to increase the cell constant.

This material is based upon work supported by the National Key R&D Program of China (No. 2017YFA0304203), the National Natural Science Foundation of China (Nos. 61622503, 61575113, and 11434007), and the Changjiang Scholars and Innovative Research Team in the University of Ministry of Education of China (No. IRT13076). Frank Tittel acknowledges the support by the National Science Foundation (NSF) ERC MIRTHE award and the Robert Welch Foundation (Grant No. C-0586).

[1]J. Luo, Y. Fang, Y. Zhao, A. Wang, D. Li, Y. Li, Y. Liu, F. Cui, J. Wu, and J. Liu, Anal. Methods **7**, 1200 (2015).
[2]X. Zhang, B. Yang, X. Wang, and C. Luo, Sensors **12**, 9375 (2012).
[3]H. Dai, P. Xiao, and Q. Lou, Phys. Status Solidi A **208**, 1714 (2011).
[4]L. Dong, A. A. Kosterev, D. Thomazy, and F. K. Tittel, Appl. Phys. B **100**, 627 (2010).
[5]H. Yi, K. Liu, W. Chen, T. Tan, L. Wang, and X. Gao, Opt. Lett. **36**, 481 (2011).
[6]H. Zheng, L. Dong, A. Sampaolo, P. Patimisco, W. Ma, L. Zhang, W. Yin, L. Xiao, V. Spagnolo, S. Jia, and F. K. Tittel, Appl. Phys. Lett. **109**, 111103 (2016).
[7]A. A. Kosterev, L. Dong, D. Thomazy, F. K. Tittel, and S. Overby, Appl. Phys. B **101**, 649 (2010).
[8]X. Yin, L. Dong, H. Zheng, X. Liu, H. Wu, Y. Yang, W. Ma, L. Zhang, W. Yin, L. Xiao, and S. Jia, Sensors **16**, 162 (2016).
[9]Y. Ma, Y. He, L. Zhang, X. Yu, J. Zhang, R. Sun, and F. K. Tittel, Appl. Phys. Lett. **110**, 031107 (2017).
[10]Z. Wang, Q. Wang, J. Y. Ching, J. C. Wu, G. Zhang, and W. Ren, Sens. Actuators, B **246**, 710 (2017).
[11]K. Liu, X. Guo, H. Yi, W. Chen, W. Zhang, and X. Gao, Opt. Lett. **34**, 1594 (2009).
[12]H. Wu, L. Dong, H. Zheng, Y. Yu, W. Ma, L. Zhang, W. Yin, L. Xiao, S. Jia, and F. K. Tittel, Nat. Commun. **8**, 15331 (2017).
[13]A. Szabó, Á. Mohácsi, G. Gulyás, Z. Bozóki, and G. Szabó, Meas. Sci. Technol. **24**, 065501 (2013).
[14]S. Viciani, M. Siciliani de Cumis, S. Borri, P. Patimisco, A. Sampaolo, G. Scamarcio, P. De Natale, F. D'Amato, and V. Spagnolo, Appl. Phys. B **119**, 21 (2015).
[15]M. Siciliani de Cumis, S. Viciani, S. Borri, P. Patimisco, A. Sampaolo, G. Scamarcio, P. De Natale, F. D'Amato, and V. Spagnolo, Opt. Express **22**, 28222 (2014).
[16]V. Spagnolo, P. Patimisco, R. Pennetta, A. Sampaolo, G. Scamarcio, M. S. Vitiello, and F. K. Tittel, Opt. Express **23**, 7574 (2015).
[17]H. Wu, L. Dong, H. Zheng, X. Liu, X. Yin, W. Ma, L. Zhang, W. Yin, S. Jia, and F. K. Tittel, Sens. Actuators, B **221**, 666 (2015).
[18]H. Wu, A. Sampaolo, L. Dong, P. Patimisco, X. Liu, H. Zheng, X. Yin, W. Ma, L. Zhang, W. Yin, V. Spagnolo, S. Jia, and F. K. Tittel, Appl. Phys. Lett. **107**, 111104 (2015).
[19]P. Patimisco, G. Scamarcio, F. K. Tittel, and V. Spagnolo, Sensors **14**, 6165 (2014).
[20]J. P. Besson, S. Schilt, and L. Thévenaz, Spectrochim. Acta, A **60**, 3449 (2004).
[21]A. Karbach and P. Hess, J. Chem. Phys. **83**, 1075 (1985).
[22]A. Miklós, P. Hess, and Z. Bozóki, Rev. Sci. Instrum. **72**, 1937 (2001).
[23]X. Yin, L. Dong, H. Wu, H. Zheng, W. Ma, L. Zhang, W. Yin, S. Jia, and F. Tittel, Sens. Actuators, B **247**, 329 (2017).
[24]See http://www.hitran.com for HITRAN Database for the information about the spectral line parameter.